Local characterization of rare-earth-doped single microspheres by combined microtransmission and microphotoluminescence techniques

Daniel Navarro-Urrios,[1,2,*] Marta Baselga,[2] Federico Ferrarese Lupi,[2] Leopoldo L. Martín,[3] Carla Pérez-Rodríguez,[3] Víctor Lavin,[3] Inocencio R. Martín,[3] Blas Garrido,[2] and Néstor E. Capuj[4]

[1]*Catalan Institute of Nanotechnology (ICN), Campus UAB, Edifici CM3, Bellaterra 08193, Spain*
[2]*MIND-IN2UB, Departamento de Electrònica, Universitat de Barcelona, C/Martí i Franquès 1, Barcelona 08028, Spain*
[3]*Departamento de Física Fundamental y Experimental, Electrónica y Sistemas and MALTA Consolider Team, Universidad de La Laguna, Tenerife 38206, Spain*
[4]*Departamento de Física Básica, Universidad de La Laguna, Tenerife 38206, Spain*
**Corresponding author: dnavarro@icn.cat*

Received June 26, 2012; revised October 5, 2012; accepted October 11, 2012; posted October 15, 2012 (Doc. ID 171427); published November 16, 2012

We present the optical characterization of single light emitting glass microspheres by means of an experimental setup that combines μ-transmission and μ-photoluminescence measurements without the need of optical fibers for excitation or detection purposes. We demonstrate that the results provided by both techniques are consistent among them and can provide complementary information regarding the active material properties (material losses and cross sections) and the passive resonator ones (radiative quality factors, group refractive indices, sphere radius, and pump power threshold for mode spectral shifting). This work addresses Nd^{3+} doped borate glass microspheres, but the reported studies could be realized in other rare-earth-doped glass microspheres as well.

OCIS codes: 300.0300, 180.0180.

1. INTRODUCTION

Optical microsphere resonators have been used extensively in fundamental research such as cavity-QED studies and applied research such as optoelectronics [1–3]. As an optical system, they behave as high quality factor (Q) cavities, supporting the so-called whispering gallery modes (WGMs). WGMs are specific eigensolutions of the Maxwell equations in which the electromagnetic field is pressed down to the sphere surface without any roots inside the sphere [4]. During the last years the sensing applications, in particular biochemical, of microspheres have drawn increasing attention [5–8], since the spectral position of the WGMs is very sensitive upon changes of the refractive index of the surrounding medium.

The first experimental studies reporting WGMs on single microsphere-like structures were done already three decades ago on levitating liquid droplets of aerosols (observed by means of elastic and inelastic scattering of free-space beams) [9]. However, efficient and robust external excitation of high-quality WGMs supported by a single microsphere is an issue for their practical applications. Indeed, the first commercial WGM resonator-based devices have been achieved only after the successful development of waveguide coupling techniques [10].

Microspheres composed by a light emitting material present the clear advantage over passive ones that WGMs are directly excited by the spontaneous or stimulated emission of the material if the wave vector and physical position of the emitter overlap with the wave vector and the energy distribution of the mode respectively. Main issues on these structures are the achievement of an efficient pumping of the emitting species and the increased optical losses that active materials frequently show with respect to passive ones. When aiming to sensing applications, WGMs spectral shifting associated with pump-induced local temperature increasing is also a subject to be addressed [11].

On light emitting microspheres it is interesting to combine transmission and photoluminescence (PL) measurements on because of their complementarity. Indeed, the first technique provides information about the material in its fundamental state and on the absence of local heating. Moreover, as it will be revealed later, apart from the appearance of WGMs associated dips in transmission, there is an oscillating-like behavior that can provide further information about the radius of the microspheres if its material refractive index is known. On the other hand, a μ-PL technique provides much more intense WGMs signal contribution if the resonator contains an efficient emitter and allows testing some of its active properties and potentialities, e.g., absorption and emission cross sections (the latter could be enhanced by the Purcell effect occurring in optical cavities [12], lasing action, and optomechanical features). To ensure that the pump power does not influence the spectral WGM position due to local thermal heating, the direct comparison with a μ-transmission measurement can be very useful.

One of the main drawbacks of spherical microresonators is that, under the conventional fabrication techniques, it is very unlikely to produce perfect spheres, most probably obtaining spheroid shapes. This translates into WGM spectra that

depend on the specific normal vector angle of the optical trajectory, which makes its optical characterization quite challenging, in particular if several different techniques are to be applied.

In this manuscript we address the issues stated above, in the particular case of single Nd^{3+} doped borate glass microspheres, by means of performing both μ-transmission and μ-PL spectra of a selected region of a given microsphere, associated with closed trajectories with similar values of the azimuth and altitude of the normal propagation vector.

2. EXPERIMENTAL SECTION

A. Fabrication

The microspheres of this study were fabricated with the method of Elliot *et al.* [13] from bulk borate glass doped with neodymium (Nd^{3+}) ions [14]. The glass is reduced to dust by means of a mortar and is heated up to its fusion temperature, which is around 900°C. Most of the splinters melt and, when the temperature decreases, solidify in a spherical shape of several micrometer radii. Aiming to facilitate the handling of the microspheres, they are deposited on a lab glass and covered by a liquid polymer. The microspheres become effectively embedded on the polymer that solidifies around them after a heating procedure. Thus, the microspheres feel a homogeneous surrounding medium with the refractive index of the polymer ($n = 1.49$).

B. Optical Characterization Setup

The experimental setup used for realizing μ-PL and μ-transmission measurements is schematized in Fig. 1. Both techniques share the same collection setup, which consists of a microscope objective (NA = 0.4) placed on a *xyz* microprecision mount. A linear polarizer is placed just after the objective on a region where the collected signal is collimated. The signal is finally focused onto the entrance slit of a 750 mm focal length monochromator coupled to a CCD camera and a photomultiplier. The whole collection system allows a maximum wavelength resolution of slightly less than 0.06 nm. By opening the entrance slit to its maximum and placing the diffraction grating of the monochromator in the zero order it is possible to build an image of the focal plane of the collection objective. This allows a first rough alignment of the position of the microspheres. Indeed, since the sample holder possess an independent *xyz* movement, it is possible to situate the region of the microspheres to be analyzed at will. By closing the entrance slit, this physical region is much reduced and the spectral resolution of the monochromator improves at the expense of a reduction of the amount of signal received. We have estimated that the lateral spatial resolution of our setup is about 5 um.

The dimensions of a given sphere have been quantified by using the collection objective of our setup and forming the sphere image on a CCD screen. This system was calibrated with a structure of known size and has an accuracy of ± 1 μm.

In order to perform the μ-PL measurements we have used the 514 nm line of an Argon laser as an excitation source, which is partially resonant with the $^4I_{9/2} \rightarrow {}^4G_{7/2}$ absorption transition of Nd^{3+} ions. The pump laser is focused on the top of a single microsphere by means of a long working distance objective, which provides a spot size of few micrometers and a power flux of 1×10^4 W/cm^2. The exact pumping place can also be independently controlled micrometrically. Contrary to what happens on a confocal microscope, the total independence among the pumping and the collection optics allows a very high freedom in terms of pumping one region of a sphere and observing another well separated from each other in the three directions of space. In the following we will present μ-PL results associated with the $^4F_{3/2} \rightarrow {}^4I_{9/2}$ radiative transition, which is a very efficient one that covers a region

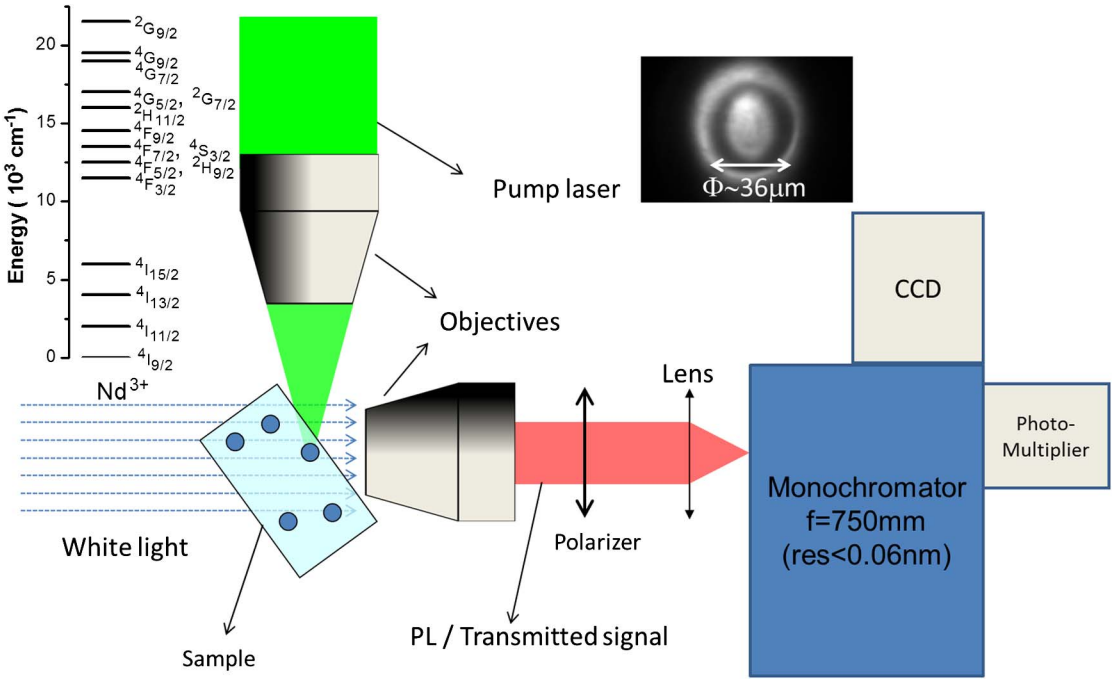

Fig. 1. (Color online) Scheme of the combined μ-transmission and μ-PL setup. Top right: image of a microsphere taken with the CCD when the monochromator is in the zero order and the slit of the monochromator widely opened. Top left: energy level structure of Nd^{3+} ion.

of several tens of nanometers around 880 nm. We have focused our study into this transition since, in this spectral region, the average dimensions of the borate glass microspheres are ideal to support WGM with high radiative Q. Since the transition involves the fundamental level it is also possible to extract information about its associated absorption cross section. A long-wave pass filter is placed in the collection stage in order to filter out the pumping laser from the PL signal.

On the other hand, μ-transmission measurements were performed by illuminating the back part of the sample with a broad band source, which, given the small dimensions of the sphere, can be considered a free plane wavefront. The setup presents the particularity of collecting the transmitted signal, not only within a reduced solid angle around the incident light direction (given by the NA of the objective), but also of a small region covering just one lateral edge of the microspheres under analysis.

Summarizing, in this combined setup it is possible to perform μ-PL or μ-transmission measurements keeping the collection and sample positions unchanged. Different parts of the microspheres can be analyzed by just displacing the sample holder.

3. RESULTS AND DISCUSSION

Within this section we will first present the μ-transmission results of an isolated microsphere, in which the different observed features are addressed. In particular we will discuss about the presence of a robust oscillating-like signal in addition to sharp resonances associated with WGM excitation. After this, we will perform a quantitative study of the different contributions to the overall quality factor of a microsphere by analyzing its spectral dependence. That study will be the basis for extracting fundamental properties of the Nd^{3+} ion within the borate glass such as its cross sections. Finally, we will address combined μ-PL and μ-transmission spectra of a reduced region of a single microsphere.

A. Optical μ-Transmission Characterization

Radiative coupling of the WGMs of a microsphere and a beam of light propagating in the external space is described in generalized Lorentz–Mie scattering theory [15], or modified ray theory described in [16]. It is, however, well known that free beams do not efficiently couple to high Q WGMs in resonators where the radius exceeds several wavelengths [17]. Indeed, such a coupling is based on a radiative energy exchange of a WGM with external space, which is negligible in the vast majority of experiments and applications with resonators exceeding few tens of micrometers in diameter. In the following we show that, by reducing the physical observation region by means of a microscope objective, the WGM signal to offset signal ratio can be greatly enhanced and transmission dips associated with WGMs emerge.

Figure 2 illustrates the previous statement. The black curve of panel (a) shows the transmission spectrum of the lab glass covered with the polymer and it roughly follows the emission spectrum of the illumination lamp. We have afterward carefully aligned a microsphere of $R = 18$ μm in a way that we just collect light coming from a reduced microsphere region around one of its lateral edges. Under these conditions the transmission spectrum becomes that represented by the gray curve,

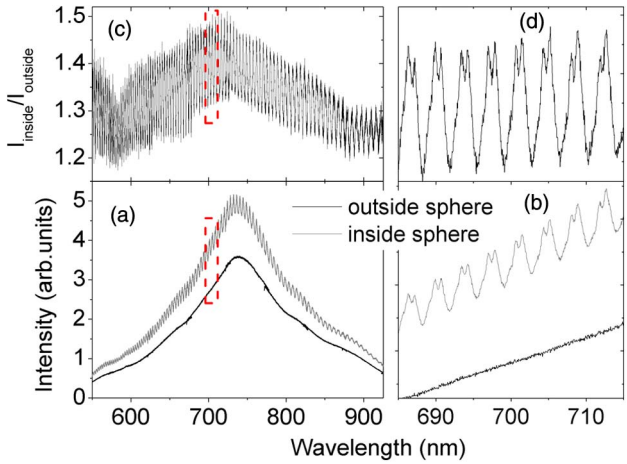

Fig. 2. (Color online) Panels (a), (b): absolute transmitted intensity when collecting light of a region around a microsphere lateral edge (gray) and of a region far away from a microsphere (black). Panels (c), (d): ratio of the curves represented on the bottom panels. Panels (b), (d) show a zoomed spectral region corresponding to the dashed red rectangle.

which has been taken by selecting the TM polarization (tangential to the sphere surface). In panel (b) we represent a zoomed region of both curves. The gray curve presents an oscillatory-like behavior and shows a higher intensity than the black curve due to what we believe is a consequence of a microlens effect. In panels (c) and (d) we show the full spectrum and a zoomed part respectively of the transmitted enhancement associated with the presence of a microsphere. The latter curve clearly presents sharp dips superimposed to the oscillatory-like behavior, which are associated with WGMs. We have observed that slight altitude displacements of the sample holder lead to a spectral shift of the WGMs positions up to 1 nm due to the asphericity of the resonator. This latter observation points out the importance of reducing the analysis region of the microsphere, in particular when a sensing application is pursued. The possibility of detecting WGM spectral features by means of a μ-transmission technique enables the characterization of the passive optical properties of the microsphere, since the ions are in the fundamental state and there is no local heating that may shift the WGM spectrum.

The ratio among the average free spectral range (FSR) of the oscillating signal and that of the WGMs is defined as Γ_{FSR} and takes a value of $\Gamma_{FSR} = FSR_{osc}/FSR_{WGM} = 1.03$ independently of the spectral region analyzed.

In order to have more insight on the oscillating-like signal we have done μ-transmission spectra of several microspheres with different radii. The spectral measurements are shown in the bottom panel of Fig. 3, where a decreasing of the FSR is observed when the microsphere radius is increased. Furthermore, in the top panel we have plotted the FSR values associated with the oscillating-like signal as a function of the radius (in log-log scale) and a $1/R$ behavior is extracted from the fit. This is a clear indication of an interference phenomenon involving light propagating within the microsphere with a shorter optical path with respect to that of the WGMs. It is worth noting that the presence of WGMs is hardly observable in this set of curves since the alignment has not been optimized for this purpose, while the oscillating-like signal appears without any special care on the illumination or collection conditions.

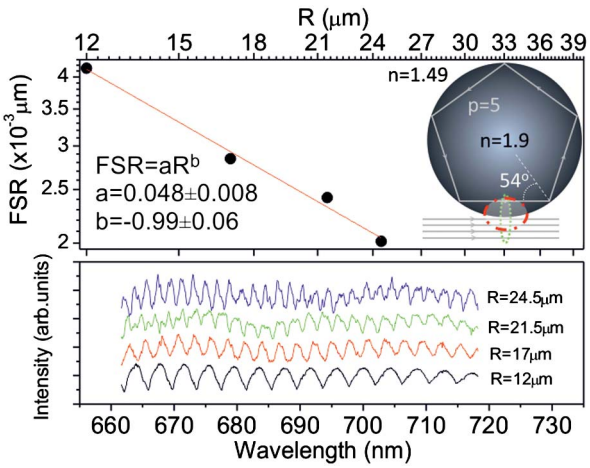

Fig. 3. (Color online) Bottom panel: μ-transmission spectra corresponding to microspheres of increasing radii. Top panel: FSR of the oscillating signal as a function of the radius of the microsphere together with a fit using a $1/R$ dependence. Inset: Schematics of the $p = 5$ optical trajectory within a microsphere. The diffracted beam (below the sphere) and a possible scenario for the coupling region for excitation of the $p = 5$ mode (dashed-dotted) and observation region (dotted) are also shown.

On the basis of the previous observations, we explain the oscillating-like signal within a geometrical optics framework, in which low quality factor modes are excited. Indeed, we have excluded diffraction effects because of the small FSR detected. Given the particular experimental conditions already stated above in the manuscript (a low collection solid angle and a reduced microsphere region under analysis) and the small difference among the FSR of the oscillating signal and that of the WGMs we also discard the possibility of interference among refracted (even after several internal reflections) and diffracted light.

Instead, we think that we are exciting relatively low-order Mie modes of the microsphere that can be also interpreted with a simple geometrical model (schematized in the inset of Fig. 3). The incident light partially couples inside the microsphere by evanescent coupling, afterward propagating on a closed polygonal-like trajectory. If the optical path within the microsphere is an integer multiple m of the wavelength ($m\lambda = nd$), a resonant standing wave will be excited, with $\mathrm{FSR}_{\mathrm{osc}} = (1/n_g)(\bar{\lambda}^2/d)$, where $\bar{\lambda}$ is the average wavelength between two adjacent resonances and n_g is the group refractive index. If we define p as the number of reflections inside the microsphere, $p = 3$–4 cannot store much energy within the microspheres because those trajectories do not fulfill the condition of total internal reflection and thus most of the coupled light will be radiated just by refraction. In fact, given the refractive indices of the microsphere ($n = 1.9$) and the embedding medium ($n = 1.49$), the critical angle for total internal reflection within the microsphere is about 52°. Only in closed trajectories with $p \geq 5$ the internal incident angles are above that critical angle value, thus being able to accumulate enough energy to provide a sizeable effect in a transmission measurement. This occurs since, even though the Q factors associated with these modes ($Q \sim 10^2$) reveal high radiative losses when compared to those shown by the WGMs ($Q \sim 10^3$–10^4), the same reason allows to couple in light much easier. It is worth noting that it was also possible to obtain reasonably good results by using a freely available software that uses a standard Mie scattering theory code [18], which is the most rigorous way to describe the scattering of a plane wave by a homogeneous sphere and incorporates all the possible modes supported by the sphere. However, this theory does not fit our experimental conditions, since, on the one hand, we measure the relative transmission and, on the other hand, it turns out that the coupling to those low quality factor modes is a dominant feature over other contributions. This latter observation is likely associated with our particular experimental conditions, since we are testing the contribution of a reduced region of the whole sphere onto a small solid angle given by the collection objective. As it was stated before, the experimental value of the ratio among the FSR of the oscillating signal and that of the WGMs was $\Gamma_{\mathrm{FSR}} \sim 1.03$, which agrees with that given theoretically by a closed trajectory with $p = 5$ with an optical path of $d = 10R \cos 54°$. Indeed, $\Gamma_{\mathrm{FSR}} = \mathrm{FSR}_{\mathrm{osc}}/\mathrm{FSR}_{\mathrm{WGM}} = 2n_{\mathrm{wgm}}R\pi/10nR \cos 54° = 1.04$, where n_{wgm} is the group refractive index of the WGMs and, as it will be shown afterward, it has been measured to be $n_{\mathrm{wgm}} = 1.84$. By inserting the measured material refractive index of the microsphere on the FSR formula, we can extract an indirect value of $R = 17.3$ μm, which is compatible with the value determined from the CCD image. This simple way of extracting the radius of the sphere is quite robust against changes in the material refractive of the surrounding medium, since, under the geometrical optics approximation, it only depends on the material refractive index of the sphere and on the order of the supported polygonal trajectory.

B. μ-PL Characterization

In this subsection we will present a quantitative analysis of the spectral behavior of the quality factor (Q) using the μ-PL technique. Such study will provide useful information of the optical loss associated with the dopant as well as of the geometrical properties of the resonator.

In the bottom panel of Fig. 4 we show a highly resolved TM-polarized μ-PL high resolution spectrum ($\Delta\lambda < 0.06$ nm) corresponding to a μ-sphere of $R = 13$ μm, covering the $^4\mathrm{F}_{3/2} \rightarrow {}^4\mathrm{I}_{11/2}$ radiative transition. Very narrow PL peaks associated with WGM appear superimposed to an offset signal coming from emitted light that was not coupled to the supported WGMs. In order to check for an enhancement of the spontaneous emission probability at the resonant wavelengths (which would lead to an emission cross section enhancement) we have

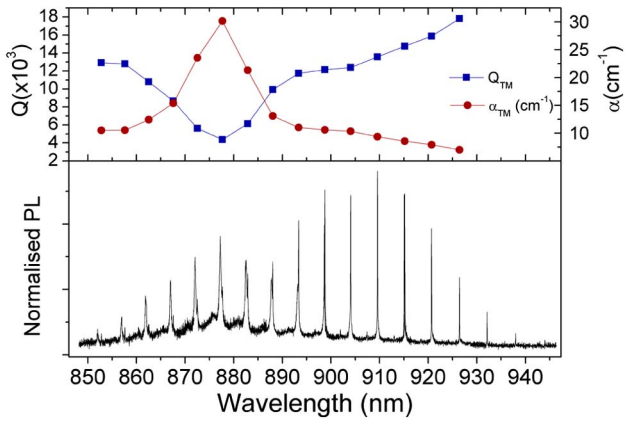

Fig. 4. (Color online) Bottom panel: μ-PL spectrum of a microspheres of $R = 13$ μm. Top panel: quality factors (squares) and extracted optical losses (circles).

performed time-resolved measurements collecting light resonant and not resonant with a PL WGM. However, we have not observed any significant difference on the lifetime (~20 μs), which was equal to that of the bulk emission. We believe that the reason of this lies in the natural widths of the Nd^{3+} optical transitions, which are much wider than that of the resonances at room temperature [19]. Thus, the presence of the cavity does not influence the dynamics of the recombination mechanisms but just selectively filters the PL emission.

From the definition of Q it is straightforward to deduce a relationship among Q, n_{wgm}, the WGM resonant wavelength (λ), and the standard loss coefficient (α) in the form of $\alpha = 2\pi n_{wgm}/Q\lambda$. It is also very useful to express the quality factor as $Q = \lambda/\Delta\lambda$, which allows its experimental determination from a continuous wave PL spectrum. Following this latter procedure, we have extracted the spectral dependence of Q, which is shown in the top panel of Fig. 4 (blue squares). A minimum value of Q of about 4×10^3 is observed around 880 nm, while a maximum value of about 18×10^3 (limited by the resolution of our setup) is obtained around 930 nm. This behavior is a consequence of the spectral dependence of the absorption losses of Nd^{3+} ions performing the $^4I_{9/2} \rightarrow {}^4F_{3/2}$ transition. In fact, relatively high losses are expected since that transition occurs from the fundamental level, which can be approximated to be fully populated at those pump fluxes. Therefore, material absorption losses totally dominate over geometrical and scattering contributions and we can establish a lower limit to the overall quality factor associated with those contributions of about 18×10^3. A further consequence of the particular spectral behavior of the losses within the visible transition is that the intensity associated with the WGM peaks finds its maximum around 910 nm, which happens at longer wavelengths with respect to the maximum of the offset PL signal associated with the bulk emission.

It is also possible to determine experimentally n_{wgm}, since it is directly related to the FSR_{WGM} of the cavity by the relation $n_{wgm} = (1/FSR_{WGM})(\bar{\lambda}^2/2\pi R)$. Using the values of FSR_{WGM} and R determined experimentally, we have obtained that n_{wgm} is about 1.84. This value is reasonable taking into account the material refractive indices of the glass sphere (1.9) and polymer cladding (1.49). Once n_{wgm} is known, it is possible to extract the associated losses of the cavity, which, for the visible region reproduce the absorption losses of the material. Standard transmission measurements on bulk samples presented similar losses values. Having the absorption losses values it is straightforward to extract the spectral behavior of the absorption cross section of the $^4I_{9/2} \rightarrow {}^4F_{3/2}$ transition, given the dopant concentration that is present within the glass. A maximum absorption cross section of $\sigma_{abs} = 1.1 \times 10^{-20}$ cm^2 has been determined at 878 nm. It is worth noting that the average error on the determination of the FWHM of a resonance is slightly higher than 1 pm, which translates into sensitivities to optical losses changes of about 0.1 cm^{-1}. Therefore, we believe that this technique may also be of use for performing excited-state absorption (ESA) spectroscopy among excited levels, since the optical pumping powers required for achieving measurable excited-state populations would be very much reduced in comparison with those used in standard ESA spectroscopy on bulk materials [20,21].

Figure 5 represents the results obtained for the same sphere when collecting light from two different physical regions (two different specific normal vector angles of the optical trajectory). The black curve corresponds to the data already shown in Fig. 4, where losses are totally dominated by material absorption. On the contrary, the red curve presents much lower quality factors. This decrease in Q is clearly associated with an increase of the passive optical losses of the sphere, i.e., those not associated with material absorption, and probably due to the slight asphericity of the resonators or a local defect on its surface. The total Q of that curve on the spectral region outside the main contribution of the absorption losses arrives to a maximum of about 5.5×10^3, which is the Q associated just with passive losses for the second trajectory. On the green curve we show the total Q calculated by combining the latter value with those associated with absorption losses (black curve). The resulting curve fits reasonably well with the red curve. We can thus conclude that the absorption losses are independent of the mode-specific propagation trajectory but the passive losses can present different values depending on the trajectory of the mode. The latter observation points out the importance of analyzing a reduced region of the microsphere.

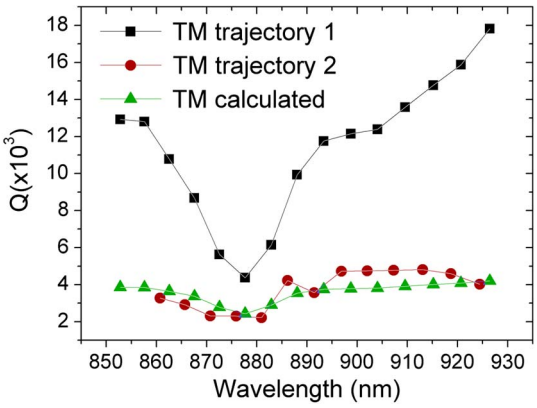

Fig. 5. (Color online) Quality factor spectrum for two different trajectories of the same sphere. A calculated curve using the material losses of the first trajectory and the radiative losses of the second is also shown.

C. Combined μ-PL and μ-Transmission Measurements

We now illustrate the consistency of μ-transmission and μ-PL techniques in our setup. In Fig. 6, we show the comparison of both spectral curves (μ-transmission is already normalized by the transmission signal obtained without microsphere) for the case of a microsphere of $R = 9.5$ μm. As shown above, the μ-transmission spectra (black curves) consist of oscillating-like signals with sharp signal dips superimposed to them that are associated with WGMs. On the other hand, the μ-PL spectrum is generated by the radiative recombination of optically pumped Nd^{3+} ions and, as stated above, show very sharp peaks associated with PL signal exciting the WGMs of the microcavity. It is remarkable the agreement in the WGMs spectral positions shown by both techniques for both polarizations. Similar combined measurements have been recently been reported on porous silicon microspheres [22], in which the authors associate the observed dips in μ-transmission with the peaks in the μ-PL spectrum. However, in [22] the position of the WGMs in the μ-PL measurements do not fit well with the dips observed on the μ-transmission measurement, which are also largely broader. We are of the opinion that what is

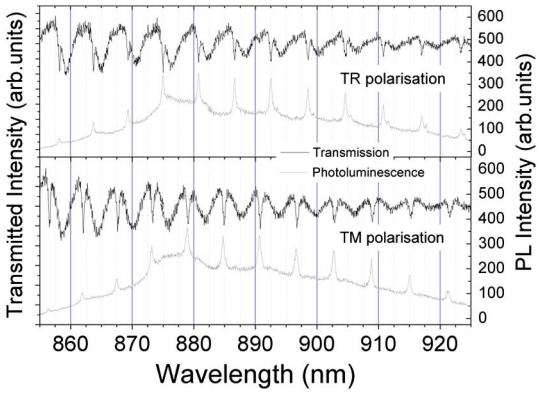

Fig. 6. (Color online) μ-PL (gray) and μ-transmission (black) measurements for TM (bottom panel) and TR (top panel) polarizations for a microspheres of $R = 9.5$ μm.

identified as WGMs in μ-transmission in [22] indeed correspond to the oscillating-like signal described above and that the transmission spectrum does not show the same WGMs observable on the PL measurement, otherwise they should coincide and show similar quality factors. Those latter observations are clearly evidenced in Fig. 6 and point out that there is no sizeable effect on the microsphere modal structure due to the presence of the pump over the microsphere. However, we have observed that increasing the pump power by less than a factor of 2 translates into a blueshifting of several tenths of nanometers the mode spectral positions, which is associated mainly with a refractive index decreasing of the polymer due to local heating effects.

Even if the WGMs on the transmitted signal are clearly observable, the intensity (with respect to the offset) associated with the WGMs generated by PL is several orders of magnitude stronger. This is one reason that supports why PL WGMs look more appealing for sensing purposes, once calibrated the maximum usable pumping power without affecting the spectral modal structure of the microsphere.

4. CONCLUSIONS

We have done combined μ-transmission and μ-PL spectra of a reduced physical region of single rare-earth-doped glass microsphere. We have demonstrated that in μ-transmission it is possible to obtain significant WGM coupling efficiency even if the external beam is in free space. In addition, we have also reported a robust oscillating-like signal, explained in terms of excitation of a closed polygonal optical trajectory experimenting at least five internal reflections that allows extracting the radius of the sphere with a good accuracy. We have performed a quantitative spectral analysis of the quality factor, which has allowed extracting fundamental properties of the active material when the passive losses are not a dominant mechanism. Finally, we have also presented the comparison of the results of both techniques for a given single microsphere and demonstrated their consistency and complementarity. This cannot be achieved unless both techniques analyze the same region of the microsphere, given their usual slight deviation from sphericity. These results may enhance the insight of rare-earth-doped isolated spheres and could be applied in the sensing field, since the combination of both techniques can provide trustful information of refractive index changes on the sphere surroundings.

ACKNOWLEDGMENTS

The authors are grateful to Ministerio de Ciencia e Innovación of Spain (MICCIN) under The National Program of Materials (MAT2010-21270-C04-02), The Consolider-Ingenio 2010 Program (MALTA CSD2007-0045), to the EU-FEDER funds and to FPI of Gobierno de Canarias for their financial support. D. Navarro-Urrios acknowledges the financial support of The Generalitat de Catalunya through the Beatriu de Pinòs program and J. Gomís-Bresco for fruitful discussions.

REFERENCES

1. K. J. Vahala, "Optical microcavities," Nature **424**, 839–846 (2003).
2. R. K. Chang and A. J. Campillo, *Optical Processes in Microcavities* (World Scientific, 1996).
3. V. S. Ilchenko and A. B. Matsko, "Optical resonators with whispering-gallery modes—Part II: Applications," IEEE J. Sel. Top. Quantum Electron. **12**, 15–32 (2006).
4. A. N. Oraevsky, "Whispering gallery waves," Quantum Electron. **32**, 377–400 (2002).
5. Biophotonics/Optical Interconnects and VLSI Photonics/WBM Microcavities, 2004 Digest of the LEOS Summer Topical Meeting (IEEE, Piscataway, NJ, 2004).
6. F. Vollmer, D. Braun, and A. Libchaber, "Protein detection by optical shift of a resonant microcavity," Appl. Phys. Lett. **80**, 4057–4059 (2002).
7. F. Vollmer, S. Arnold, D. Braun, I. Teraoka, and A. Libchaber, "Multiplexed DNA quantification by spectroscopic shift of two microsphere cavities," Biophys. J. **85**, 1974–1979 (2003).
8. J. L. Nadeau, V. S. Ilchenko, D. Kossokovski, G. H. Bearman, and L. Maleki, "High-*Q* whispering-gallery mode sensor in liquids," Proc. SPIE **4629**, 172–180 (2002).
9. A. Ashkin and J. M. Dziedzic, "Observation of optical resonances of dielectric spheres by light scattering," Appl. Opt. **20**, 1803–1814 (1981).
10. B. E. Little, S. T. Chu, P. P. Absil, J. V. Hryniewicz, F. G. Johnson, F. Seiferth, D. Gill, V. Van, O. King, and M. Trakalo, "Very high-order microring resonator filters for WDM applications," IEEE Photon. Technol. Lett. **16**, 2263–2265 (2004).
11. T. Carmon, L. Yang, and K. J. Vahala, "Dynamical thermal behavior and thermal self-stability of microcavities," Opt. Express **12**, 4742–4750 (2004).
12. E. M. Purcell, "Spontaneous emission probabilities at radio frequencies," Phys. Rev. **69**, 681 (1946).
13. G. R. Elliott, D. W. Hewak, G. S. Murugan, and J. S. Wilkinson, "Chalcogenide glass microspheres; their production, characterization and potential," Opt. Express **15**, 17542–17553 (2007).
14. L. L. Martin, P. Haro-Gonzalez, I. R. Martin, D. Navarro-Urrios, D. Alonso, C. Perez-Rodriguez, D. Jaque, and N. E. Capuj, "Whispering-gallery modes in glass microspheres: optimization of pumping in a modified confocal microscope," Opt. Lett. **36**, 615–617 (2011).
15. C. F. Bohren and D. R. Huffman, *Absorption and Scattering of Light by Small Particles* (Wiley, 1998).
16. A. Serpenguzel, S. Arnold, G. Griffel, and J. A. Lock, "Enhanced coupling to microsphere resonances with optical fibers," J. Opt. Soc. Am. B **14**, 790–795 (1997).
17. A. B. Matsko and V. S. Ilchenko, "Optical resonators with whispering-gallery modes—Part I: basics," IEEE J. Sel. Top. Quantum Electron. **12**, 3–14 (2006).
18. http://www.philiplaven.com/mieplot.htm.
19. L. A. Riseberg, "Laser-induced fluorescence-line-narrowing spectroscopy of glass: Nd," Phys. Rev. A **7** 671–678 (1973).
20. R. Reisfeld and C. K. Jorgensen, *Lasers and Excited States of Rare Earths* (Springer-Verlag, 1977).
21. B. K. Sevast'yanov, "Excited-state absorption spectroscopy of crystals doped with Cr3+, Ti3+, and Nd3+ ions. Review," Crystallogr. Rep. **48**, 989–1011 (2003).
22. F. Ramiro-Manzano, R. Fenollosa, E. Xifré-Pérez, M. Garín, and F. Meseguer, "Porous silicon microcavities based photonic barcodes," Adv. Mater. **23**, 3022–3025 (2011).